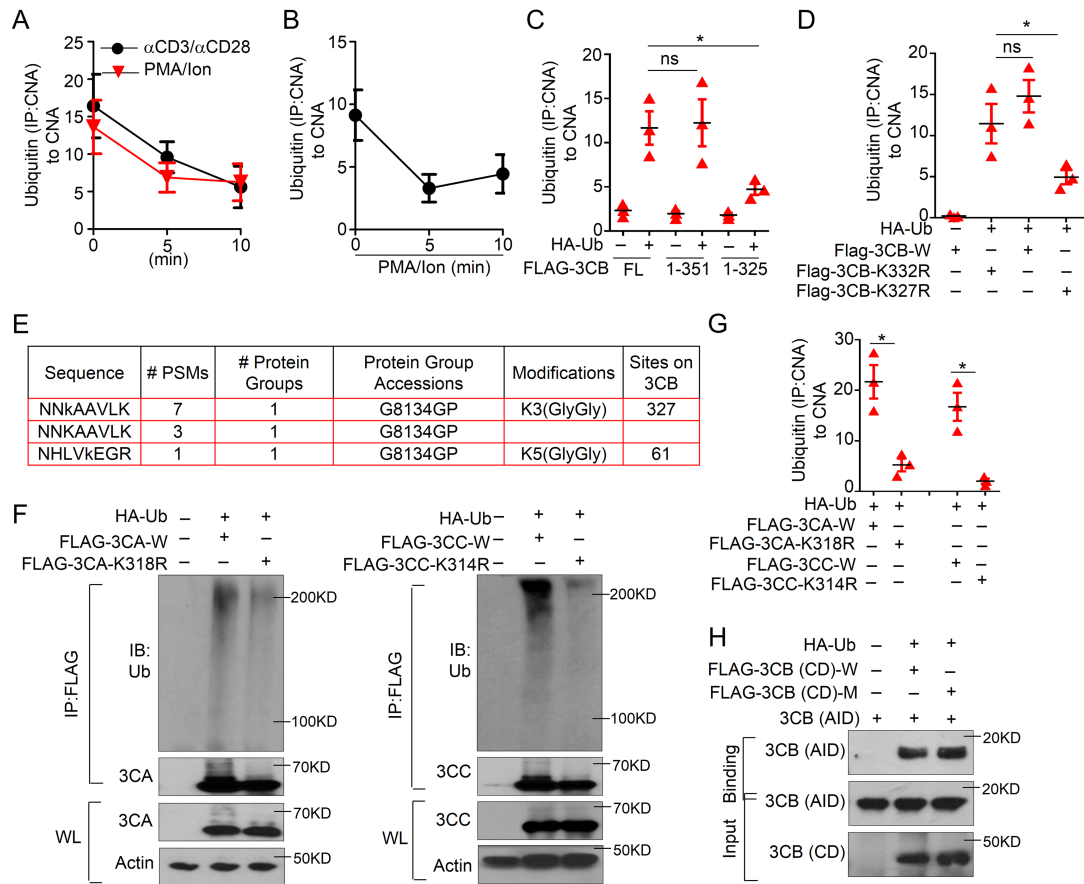
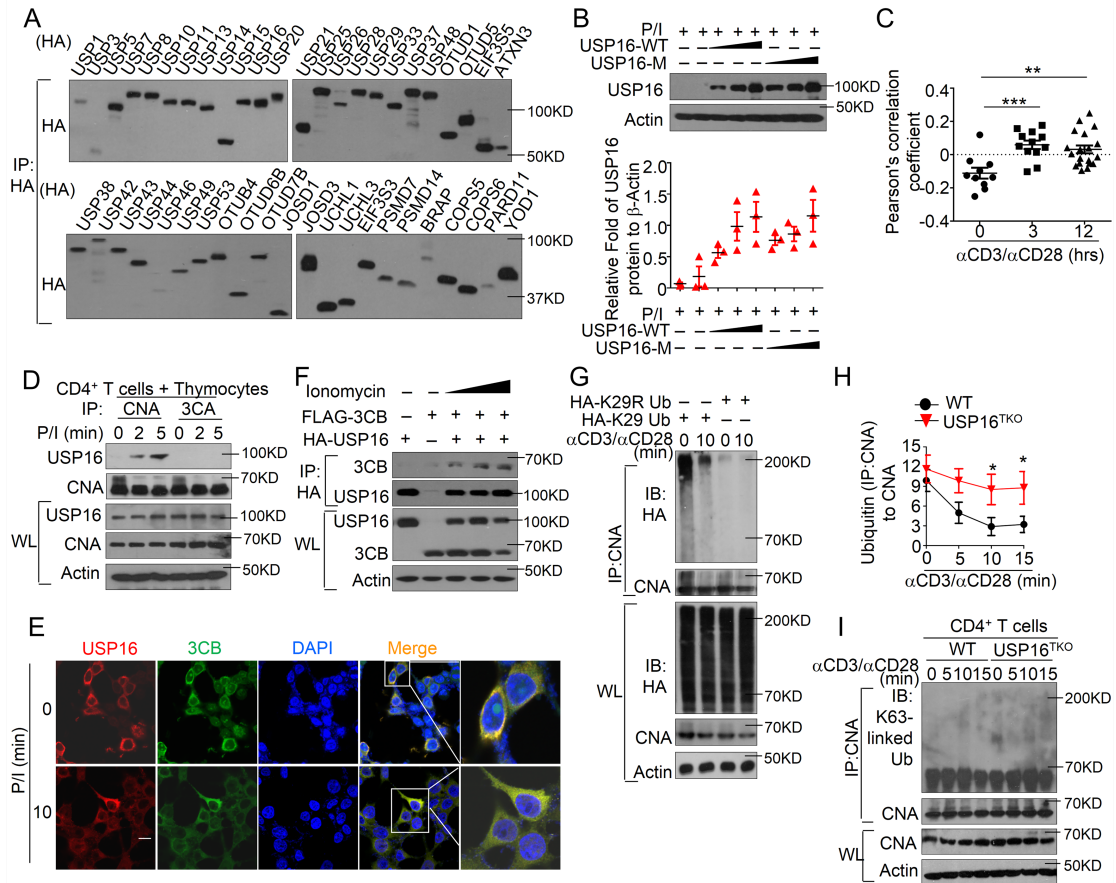


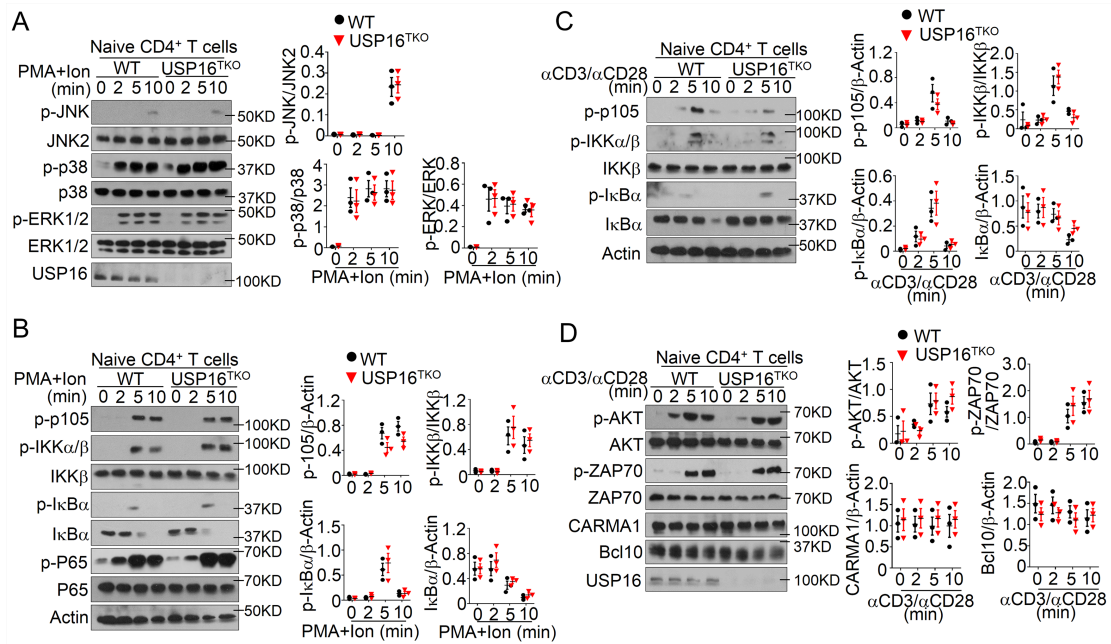
## SUPPLEMENTARY FIGURE



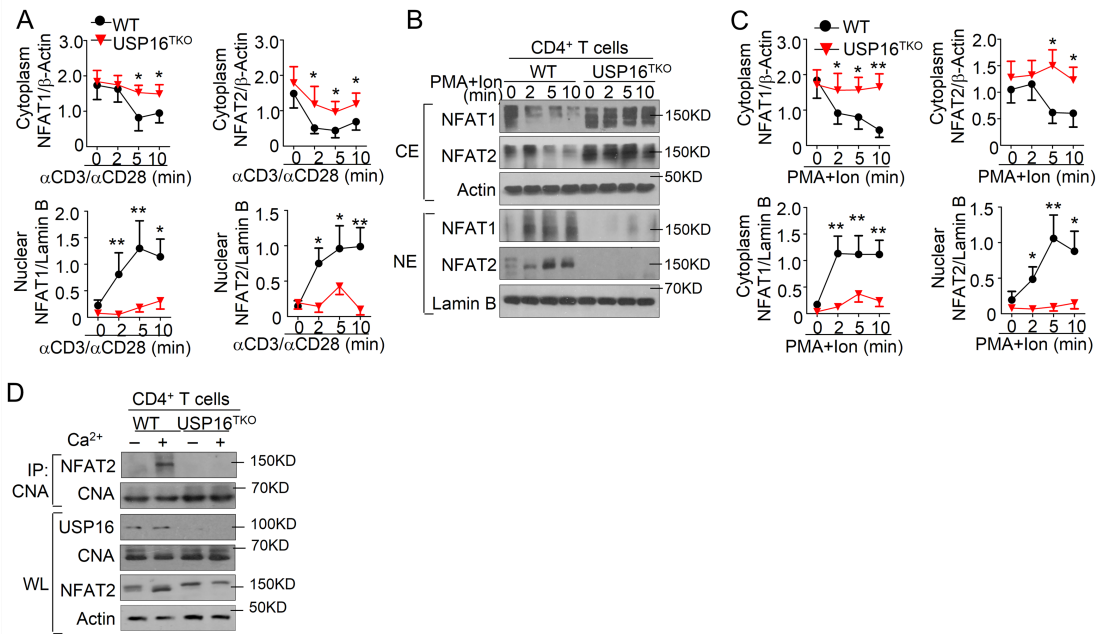
**Supplementary Figure 1 T cell activation is associated with deubiquitination of CNA.** (A) Immunoblot (IB) analysis of the ubiquitin (Ub) level of calcineurin A (CNA) in wild-type (WT) mouse splenic CD4<sup>+</sup> T cells upon  $\alpha$ CD3/ $\alpha$ CD28 or PMA/ionomycin (P/I) stimulation. (B) Human CD4<sup>+</sup> T cells isolated from the peripheral blood of healthy donors were activated with P/I. The summary graph presented relative density of ubiquitin to total CNA. (C) HEK293T cells were transfected with distinct truncations of CNA encoded by *PPP3CB* (3CB) along with WT Ub. Whole-cell lysates (WL) were subjected to immunoprecipitation (IP) using anti-FLAG followed by Ub analysis. The summary graph presented relative density of Ub to total CNA. (D) WT 3CB (3CB-W) and ubiquitination site mutants were transfected into HEK293T cells. WL were subjected to IP using anti-FLAG followed by Ub analysis. The summary graph presented relative density of Ub to total CNA. (E) CNA was isolated from mouse WT CD4<sup>+</sup> T cells by IP with anti-CNA. Ubiquitinated CNA peptide identified by mass spectrometry analysis. (F-G) Ubiquitination assay using lysates of HEK293T cells transfected with WT CNA encoded by *PPP3CA* (3CA-W), *PPP3CC* (3CC-W) or their indicated mutants along with Ub. All relative density of Ub to total CNA was calculated by using ImageJ. (H) Interaction assay of in vitro translational autoinhibitory domain (AID) with the ubiquitinated catalytic domain (CD) of WT or mutant 3CB, which was isolated from transfected HEK293T cells. The figure A-D and F-H includes the data from three independent experiments. Statistical analysis was based on three independent experiments. The error bars show mean  $\pm$  SEM. The significance of difference in (C-D) was determined by Dunnett's multiple comparisons test. The significances of differences in all other two group comparisons were determined by two-tailed Student's t test. \*, P < 0.05.



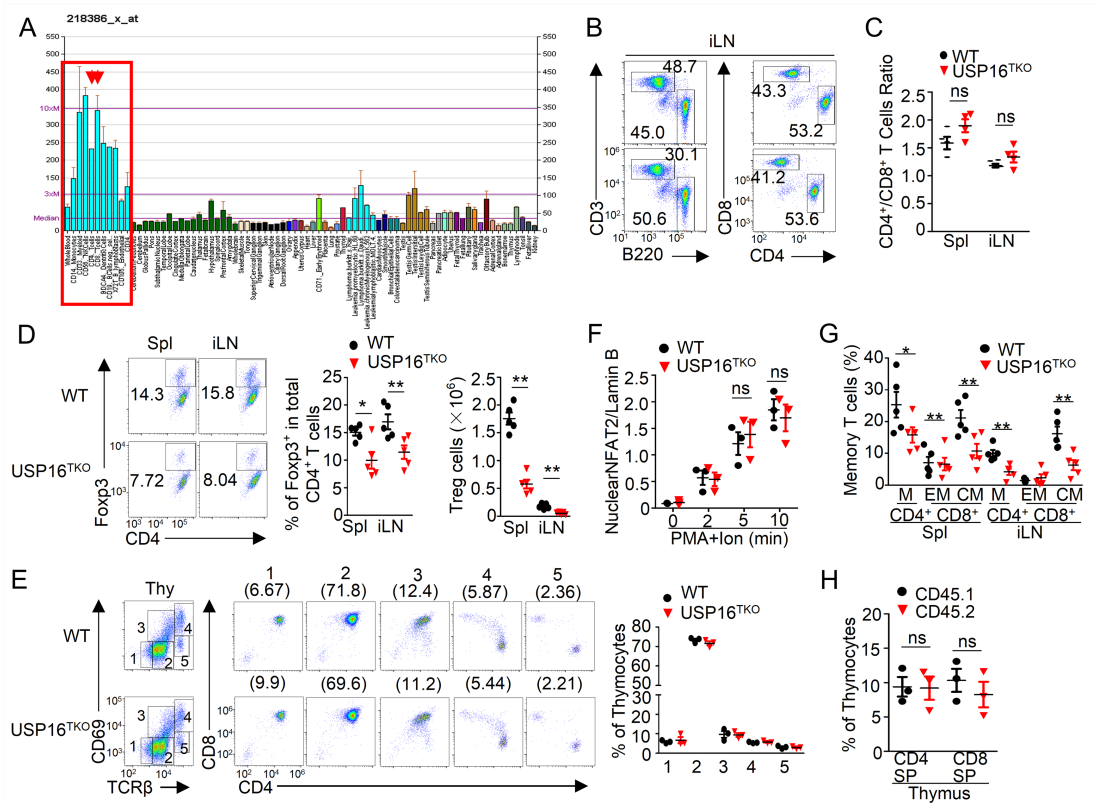
**Supplementary Figure 2 USP16 interacted with CNA and only removed K29-linked polyubiquitin chain.** (A) IB analyses of HA (pull-down HA-DUB) in main Figure 2A. (B) IB analyses of the protein levels of USP16-WT and USP16-CI in main Figure 2B. The summary graph presented relative density of USP16 to ACTIN in bottom. (C) The colocalization of CNA and USP16 in main Figure 2D was quantified as described in Materials and Methods using the Pearson's correlation coefficient ( $n > 10$ ). (D) WT peripheral CD4<sup>+</sup> T cells mixed with thymocytes, and then were stimulated with P/I as indicated. WL were subjected to IP using anti-CNA or anti-3CA, followed by IB analysis of USP16. (E) Confocal microscopy analysis of colocalization between overexpressed USP16 and 3CB in transfected HEK293T cells, which were stimulated with P/I for 10 min as indicated. The scale bars, 5 $\mu$ m. (F) HEK293T cells were transfected with indicated plasmids, and was stimulated with P/I for 10min. WL was subjected to IP using anti-HA (USP16), followed by IB analysis of FLAG (3CB). (G) WT CD4<sup>+</sup> cells were transfected with indicated plasmid using Nucleofection. After 36 h, these T cells were stimulated with  $\alpha$ CD3 plus  $\alpha$ CD28 as indication. CNA was isolated by IP using anti-CNA, followed by the detection of HA (Ub). (H) The relative level of ubiquitin to total CNA in main Figure 3G was calculated using ImageJ. (I) IB analyses of K63-linked ubiquitination of CNA in WT and USP16-deficient CD4<sup>+</sup> T cells stimulated with  $\alpha$ CD3/ $\alpha$ CD28. Data are representative of three independent experiments with three different mice in each group (C, D, H-I), three independent experiments (A, B, E, F, G). The error bars show mean  $\pm$  SEM. The significance of difference in (C) was determined by Dunnett's multiple comparisons test. \*,  $P < 0.05$ ; \*\*,  $P < 0.01$ ; \*\*\*,  $P < 0.005$ .



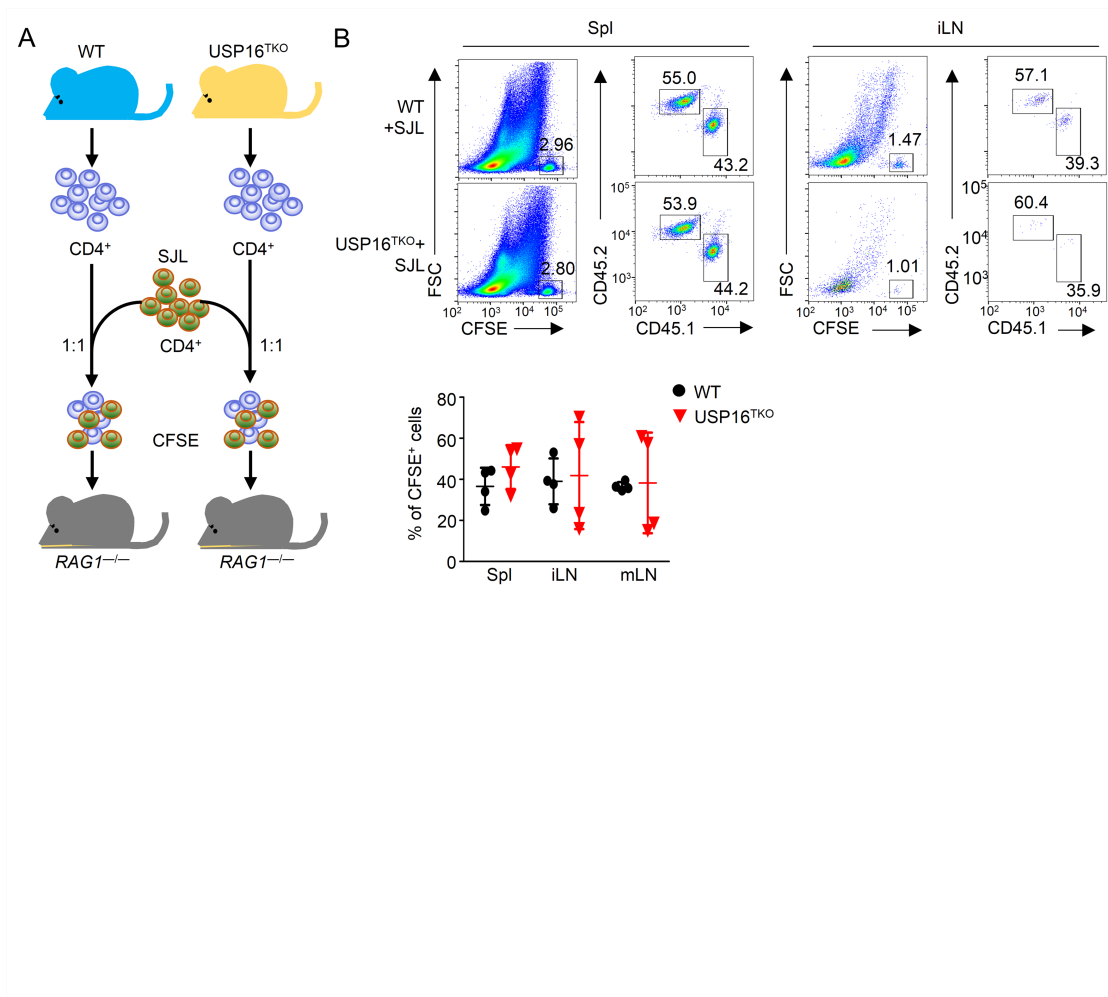
**Supplementary Figure 3 USP16 is dispensable for NF- $\kappa$ B and MAPKs activation in T cells.** (A-B) IB analyses of the proteins associated with MAPKs (A) and NF- $\kappa$ B (B) in total lysates of naive CD4<sup>+</sup> T cells (CD44<sup>lo</sup>CD62L<sup>hi</sup>) stimulated with PMA/Iono as indicated. The summary graph presented the relative density of phosphorylated protein to total input or house keeping control. (C-D) IB analyses of the canonical NF- $\kappa$ B signal (C) and TCR components (D) in naive CD4<sup>+</sup> T cells stimulated by crosslinking biotinylated  $\alpha$ CD3/ $\alpha$ CD28. The summary graph presented the relative density of phosphorylated protein to total input or house keeping control. All relative density in IB was calculated using ImageJ. Data are representative of three independent experiments with three different mice (A, B, C, D), and also presented as dot plots including all three time experiments (A-D). The error bars show mean  $\pm$  SEM. The significances of differences in two group comparisons were determined by two-tailed Student's t test.



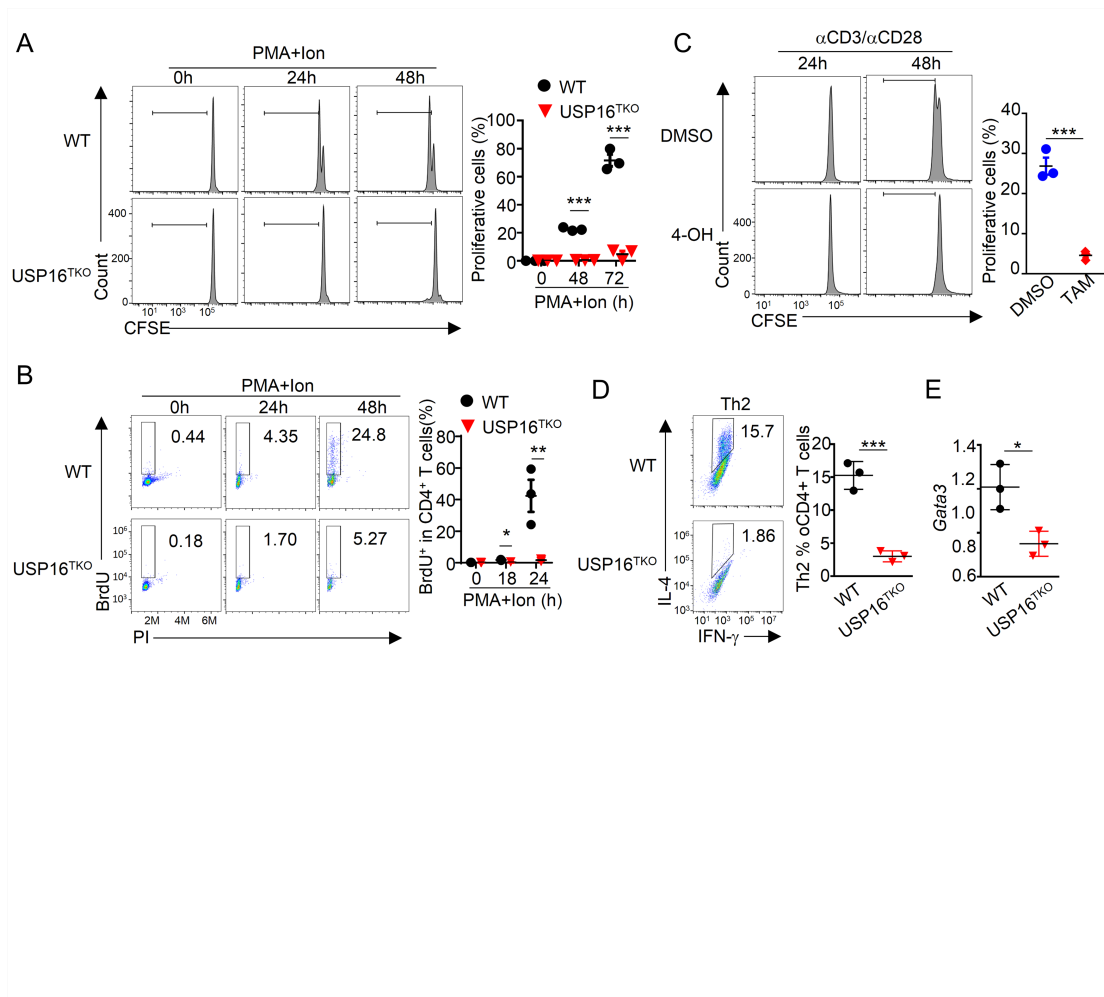
**Supplementary Figure 4 USP16 is required for activation of NFAT and its recruitment to CNA.** (A-C) IB analysis of the cytoplasmic and nuclear NFATs levels in WT and USP16-deficient CD4<sup>+</sup> T cells activated by αCD3/αCD28 (A) or PMA/Inomycin (Ino) (B-C). The summary graph presented relative density of indicated protein to housekeeping controls. (D) The interaction between CNA and NFAT2 was assessed in WT and USP16-deficient T cells activated by 2 mM CaCl<sub>2</sub>. WL were subjected to IP using anti-CNA antibody, followed by IB analyses of the associated NFAT2. All relative density in IB was calculated using ImageJ. Data are representative of three independent experiments with three different mice, and also presented as dot plots including all three time experiments (A-D). The error bars show mean ± SEM. The significances of differences in two group comparisons were determined by two-tailed Student's t test. \*, P<0.05; \*\*, P < 0.01.



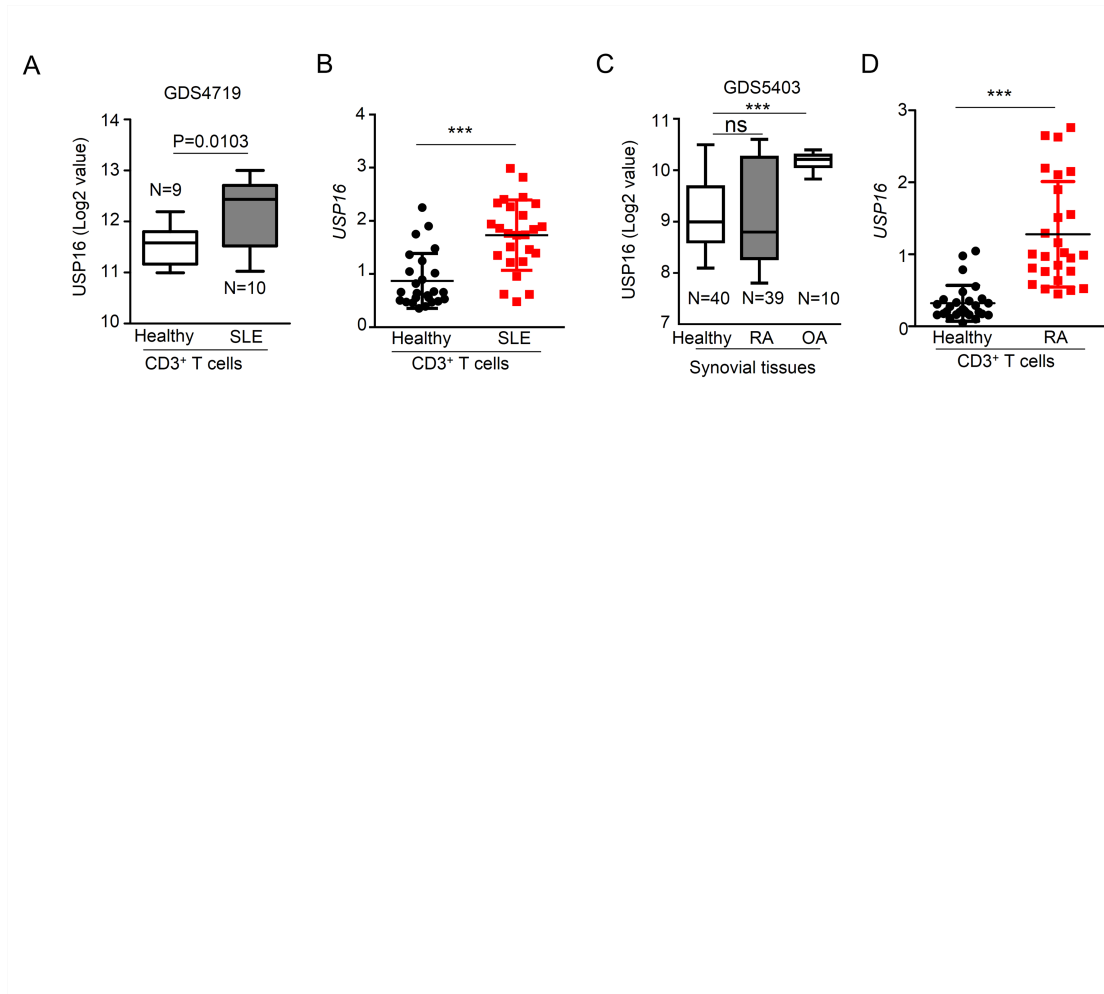
**Supplementary Figure 5 USP16 is selectively involved in peripheral T-cell maintenance.** (A) USP16 expression in distinct cell types based on BioGPS database. (B) Flow cytometric (FACS) analyses of the frequency of subpopulations of cells in the inguinal lymph nodes (iLNs) of WT and USP16<sup>TKO</sup> mice. (C) The ratio of CD4<sup>+</sup> to CD8<sup>+</sup> T cells in spleen or iLN of 6-wk-old WT and USP16<sup>TKO</sup> mice. (D) FACS analysis and summary graph of Treg cells in the spleen or iLN of 6-wk-old WT and USP16<sup>TKO</sup> mice. (E) The frequency of thymic subpopulations from 6-wk-old WT and USP16<sup>TKO</sup> mice was measured with FACS, and presented as a representative dot plots. (F) IB analysis of NFAT2 level in nucleus of WT and USP16-deficient thymocytes stimulated with P/I. The relative density of NFAT2 to Lamin B was calculated using ImageJ. (G) The frequency of T cell subpopulation in the spleen or iLNs from WT and USP16<sup>TKO</sup> mice evaluated by FACS. (H) Recombination activating gene 1 (*RAG1*)-KO recipient mice were adoptively transferred with BM cells derived from WT or USP16<sup>TKO</sup> mice (CD45.2<sup>+</sup>) along with those of B6.SJL mice (CD45.1<sup>+</sup>). Frequency of CD45.1<sup>+</sup> or CD45.2<sup>+</sup> T-cell subpopulation in the thymus was measured by FACS, and presented as a summary graph. Data are representative of three independent experiments with three different mice in each group (D-G), 4-5 independent experiments with 4-5 mice in each group respectively (B, C). The error bars show mean  $\pm$  SEM. The significances of differences in two group comparisons were determined by two-tailed Student's t test. \*,  $P < 0.05$ ; \*\*,  $P < 0.01$ .



**Supplementary Figure 6 USP16 deficiency did not affect T cell retention.** (A) Schematic diagram of the T cell retention experiment. (B) Naïve CD4<sup>+</sup> cells from 6-8 weeks old SJL (WT, CD45.1<sup>+</sup>) and USP16<sup>TKO</sup> (KO, CD45.2<sup>+</sup>) mice (female) were labeled with CFSE, and adoptively transferred into 6-8 weeks old RAG1-KO mice (female) in a mixture (at 1:1 ratio). Distribution of these CFSE-labeled T cells was analyzed 6 h later by FACS, and presented as summary graph. The figure B includes the data from three independent experiments. The error bars show mean ± SEM. The significances of differences were determined by two-tailed Student's t test.



**Supplementary Figure 7 USP16 is required for T cell proliferation.** (A) Naïve CD4<sup>+</sup> T cells were isolated from WT and USP16<sup>TKO</sup> mice by FACS sorter. These T cells were labeled with 5 μM CFSE and were stimulated with P/I as indicated. Proliferative ratio is assessed as CFSE dilution by FACS, and presented as a summary graph. (B) Cell cycle processes and genome replication of P/I-activated CD4<sup>+</sup> T cells were evaluated by bromodeoxyuridine (BrdU) staining. (C) Equal numbers of naïve USP16<sup>fllox-CreER</sup> T cells were activated with αCD3/αCD28 in the presence of DMSO or 4-hydroxy-tamoxifen (4-OH). At indicated time points after activation, the proliferation of T cells was assessed as CFSE dilution by FACS. (D-E) Naïve CD4<sup>+</sup> T cells were isolated from WT and USP16<sup>TKO</sup> mice, and were stimulated for 4 days with αCD3/αCD28 plus recombinant IL-2 (25U/ml), IL-4 (10ng/ml) and anti-IFN-γ antibodies. (D) The frequency of T cell differentiation was analyzed by FACS based on intracellular staining of the indicated cytokines. (E) qPCR analysis of *Gata3* mRNA levels in Th2-polarized WT or USP16-deficient CD4<sup>+</sup> T cells. The qRT-PCR data are presented as the fold change relative to the *Actb* mRNA level. Data are representative of three independent experiments with three mice in each group (A-D). The error bars show mean ± SEM. The significances of differences in two group comparisons were determined by two-tailed Student's t test. \*, P < 0.05; \*\*, P < 0.01; \*\*\*, P < 0.005.



**Supplementary Figure 8 High expression of USP16 is associated with autoimmune diseases.** (A) Boxplot of USP16 expression levels in healthy controls and patients with systemic lupus erythematosus (SLE) (using dataset GDS4719; n = 19). (B) qRT-PCR analysis of *USP16* mRNA level in CD3<sup>+</sup> T cells from peripheral blood of patients with SLE and healthy controls. (C) Boxplot of USP16 expression levels in healthy controls, rheumatoid arthritis (RA) and osteoarthritis (OA) patients (using dataset GDS5403; n = 89). (D) qRT-PCR analysis of *USP16* mRNA level in CD3<sup>+</sup> T cells from peripheral blood of patients with RA and healthy controls. The dot plots include three independent experiments (B, D). The error bars show mean  $\pm$  SEM. The significance of difference in (C) was determined by Dunnett's multiple comparisons test. The significances of differences in all other two group comparisons were determined by two-tailed Student's t test. \*\*\*,  $P < 0.005$ .

**Supplementary Table 1** Gene-specific primers used in qRT-PCR assay

<b>Gene</b>	<b>Forward primer</b>	<b>Reverse primer</b>
<i>Usp16</i>	CTGCCAAGACTGTAAGACTGAC	GGTGTCGTGTAGTGCTTCAAG
<i>Ifng</i>	CAGCAACAGCAAGGCGAAA	CTGGACCTGTGGGTTGTTGAC
<i>Il17a</i>	AGCGATGGTGGATGGCTCATGGTTAG	AGCTTTCCTCCGCATTGACACAG
<i>Il2</i>	CCTGAGCAGGATGGAGAATTACA	TCCAGAACATGCCGCAGAG
<i>Ppp3ca</i>	ATTGATCCCAAGTTGTCGACGAC	GCACCCTCTGTTATTATTCTCAA
<i>Ppp3cb</i>	CCATGATAGAAGTAGAAGC	TAATGTGCTTGGGTATAGAATC
<i>Ppp3cc</i>	CTTCCTCTTGCTGCCCTCTTAA	CTCGGACAGTGTGTGGGTATAGTGC
<i>Nfatc1</i>	TGTGCCGGAATCCTGAAACTC	GAGCATTTCGATGGGGTTGGAG

**Supplementary Table 2** Gene-specific primers used in vitro protein expression experiments

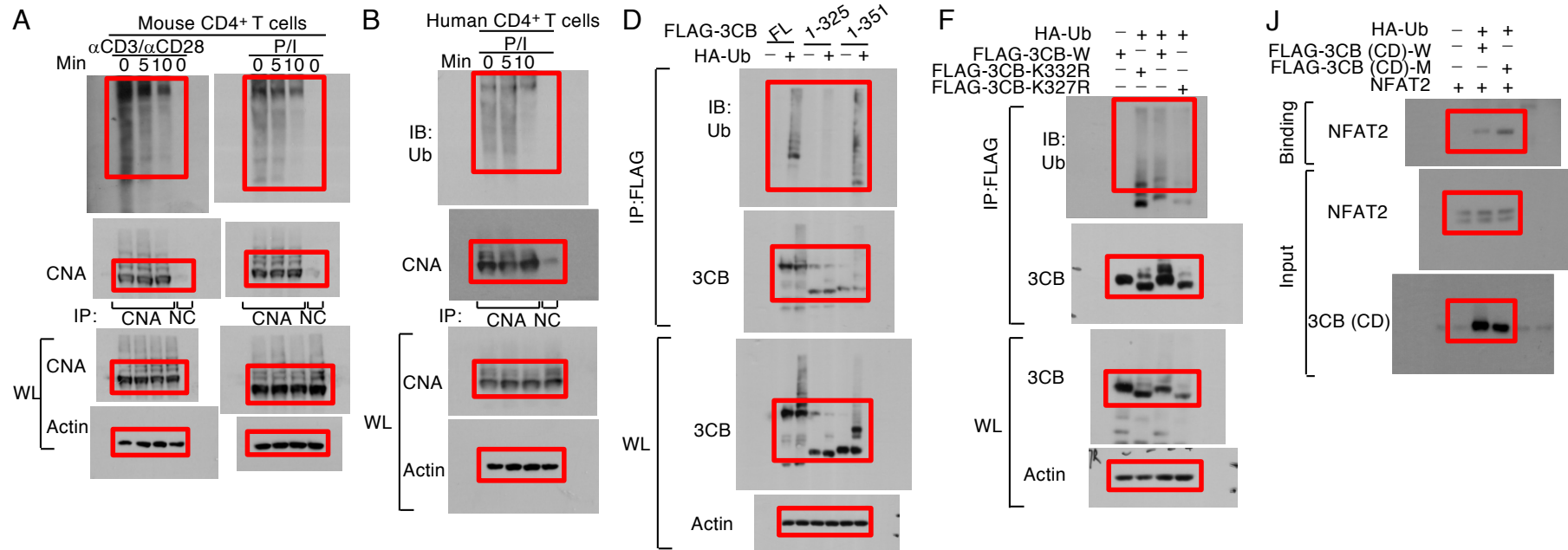
<b>Gene</b>	<b>Forward primer</b>	<b>Reverse primer</b>
<i>Usp16</i>	GGATCCATACGACTCACTATAGGGAGCCACC ATGGGAAAGAAACGGACAAAGGG	TTT TTT TTT TTT TTT TTT TTT T TTACAGTATTCTCTCATAAAAT
<i>Nfatc1</i>	GGATCC ATACGACTCACTATAGGG AGCCACCATG ATGCCAAGCACCCAGCCTTTCC AG	TTT TTT TTT TTT TTT TTT TTT T TCAGCATGGGCGAGATGGCG
<i>ppp3cb AID domain</i>	GGATCCATACGACTCACTATAGGGAGCCACC ATGATACGAGGATTCTCTCCACC	TTT TTT TTT TTT TTT TTT TTT T TCACTGGGCAGTATGGTTGCC

Accession	Description	Score	Coverage	# Unique Peptides	# Peptides	# PSMs	MW [kDa]				
G8134 GP	G8134GP	202.08	50.48	27	27	76	59.1				
A2	Sequence	# PSMs	# Protein Groups	Protein Group Accessions	Modifications	IonScore	Charge	MH+ [Da]	$\Delta$ M [ppm]	RT [min]	# Missed Cleavages
High	AAPPPPPPPPLGADR	10	1	G8134GP		59.93	2	1627.8588	-0.2451397	12.304182	0
High	NNKAAVLK	7	1	G8134GP	K3(GlyGly)	57	2	972.9479	-1.5478908	26.856789	0
High	NNKAAVLK	3	1	G8134GP		55	2	894.70584	2.8426877	29.852965	0
High	AHEAQDAGYR	2	1	G8134GP		45.8	2	1117.5026	0.4114311	6.5462059	0
High	AVFPPTHRR	4	1	G8134GP		44.52	2	1021.5577	-0.0934637	11.866813	0
High	DVVNSVGLSMGKMMAESNGTD DNSNIQ	1	1	G8134GP		33.42	4	2935.2965	0.4933726	11.451802	0
High	EEESVLTLK	2	1	G8134GP		54.34	2	1134.5889	0.0030727	14.502735	0
High	EGRVDEEIALR	2	1	G8134GP		34.76	2	1286.678	6.2523912	12.166648	1
High	FKEPPAFGPMcDLLWSDPSEDFGNE K	1	1	G8134GP	M10(Oxidation); C11(Carbamidomethyl)	47.73	3	3029.3337	0.0996973	20.983482	1
High	GFSPPHR	1	1	G8134GP		36.36	2	797.40495	-0.4721248	8.8519911	0

High	GLTPTGmLPSGVLAGGR	2	1	G8134GP	M7(Oxidation)	69.61	2	1599.85 58	2.09655 74	17.8878 7	0
High	GLTPTGMLPSGVLAGGR	2	1	G8134GP		67.79	2	1583.85 86	0.67986 28	20.1818 48	0
High	HLTEYFTFK	2	1	G8134GP		43.06	2	1185.59 38	-0.09590 24	16.0874 46	0
High	IcSFEEAK	1	1	G8134GP	C2(Carbamidomethyl)	32.51	2	983.450 55	0.24687 26	10.7576 4	0
High	IINEGAILR	4	1	G8134GP		76.79	2	1069.63 74	0.83710 64	15.1846 96	0
High	IINEGAILRR	1	1	G8134GP		20.66	3	1225.74 31	4.51634 57	13.1282 09	1
High	ILYPSTLFLLR	2	1	G8134GP		61.72	2	1335.80 42	0.53564 55	24.9620 65	0
High	RDVVNSVGLSMGKMMAESNGT DDNSNIQ	1	1	G8134GP		55.22	4	3063.39 32	1.03084 46	10.2905 97	1
High	LFEVGGSPANTR	2	1	G8134GP		50.31	2	1247.63 74	-0.45253 51	14.1196 81	0
High	LTSEEVFDMDGIPR	6	1	G8134GP		78.63	2	1590.80 12	0.08408 32	20.5357 52	0
High	MAAPEPAR	1	1	G8134GP		46.79	2	842.418 38	-0.68699 87	9.29294 47	0
High	NHLVKEGR	1	1	G8134GP	K5(GlyGly)	26.9	2	1066.57 37	-1.50228 99	2.24914 75	1
High	QTLQSATVEAIEAEK	4	1	G8134GP		89.75	2	1617.83 34	0.21035 68	16.6094 8	0

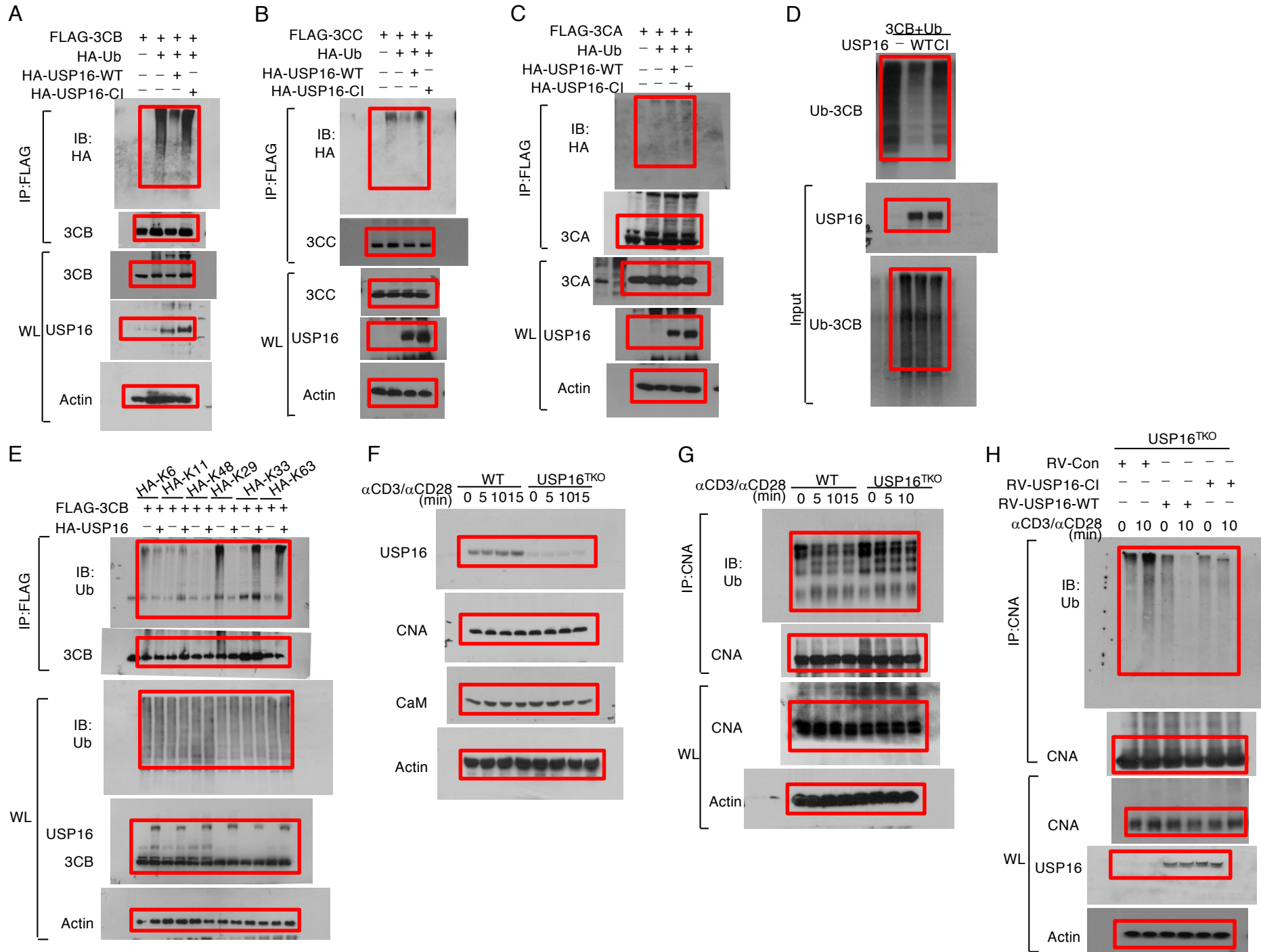
High	SQEHFSHNTVR	3	1	G8134GP		50.77	2	1341.62 94	-0.02174 22	6.69989 14	0
High	VDEEIALR	2	1	G8134GP		32.99	2	944.506 4	1.69819 39	13.1509 66	0
High	VFSVLR	3	1	G8134GP		36.15	2	720.440 05	-0.37651 97	14.9677 29	0
High	YENNVmNIR	2	1	G8134GP	M6(Oxidation)	59	2	1168.54 01	-1.27478 62	10.0983 53	0
High	YENNVmNIR	2	1	G8134GP		57.12	2	1152.54 92	2.23906 68	12.8945 74	0
High	YLFLGDYVDR	2	1	G8134GP		43.29	2	1260.62 59	-0.03903 54	20.5150 61	0

Full unedited gel for Figure 1

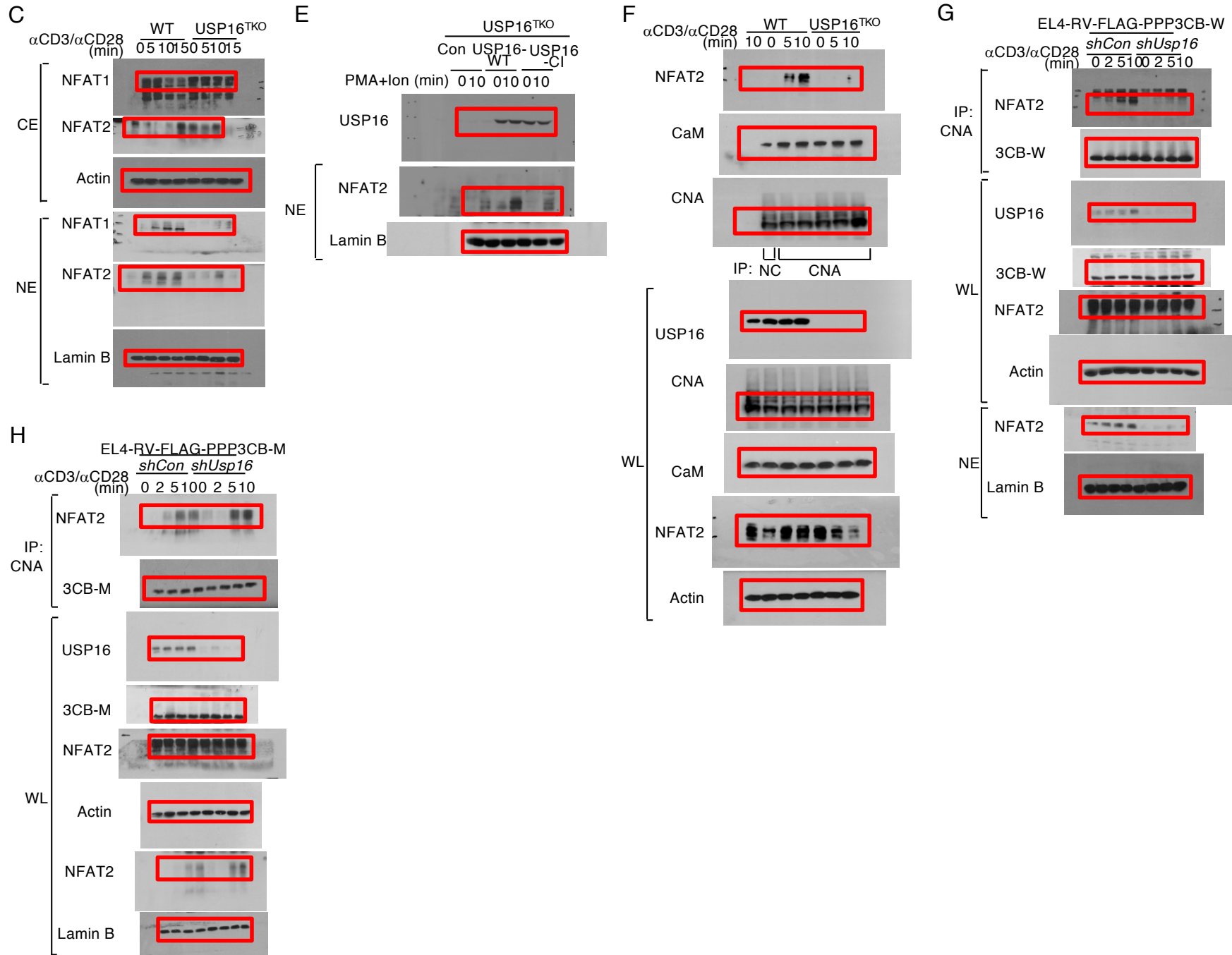




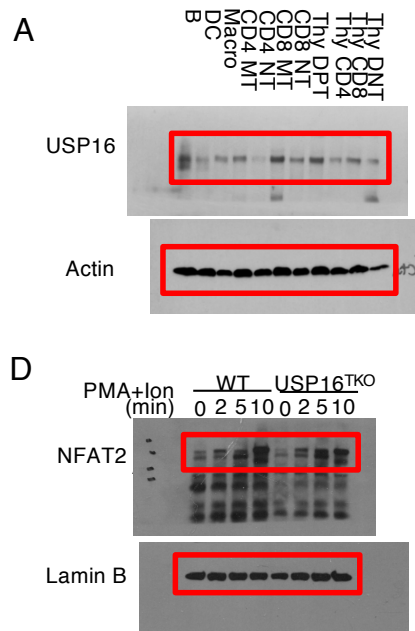
### Full unedited gel for Figure 3



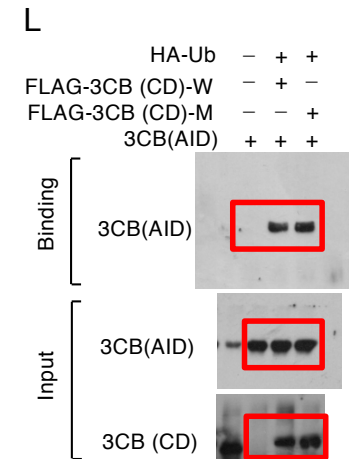
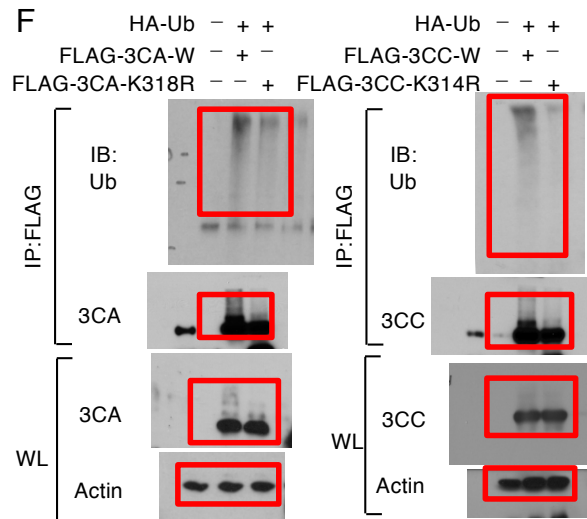
Full unedited gel for Figure 4



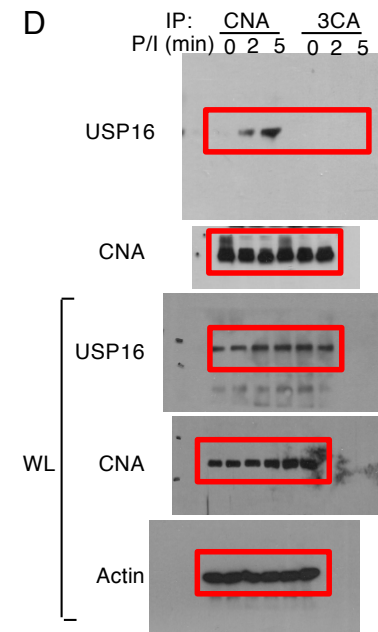
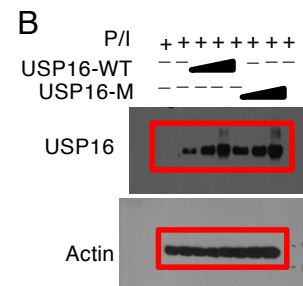
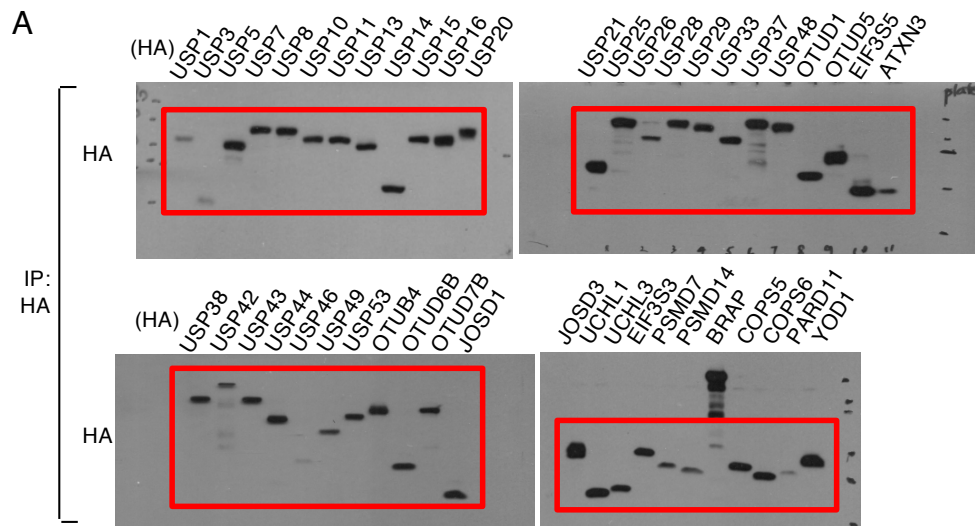
Full unedited gel for Figure 5



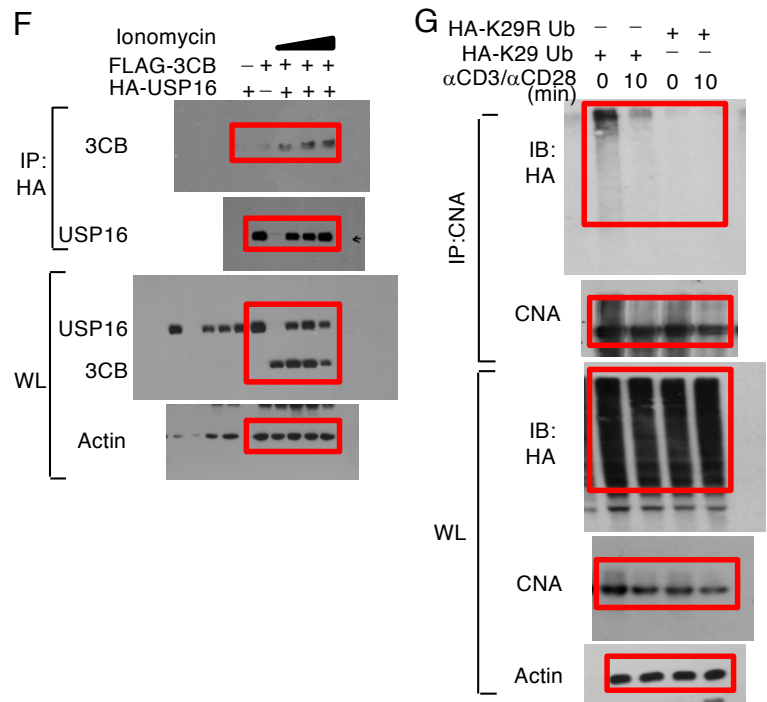
Full unedited gel for Supplementary Figure 1



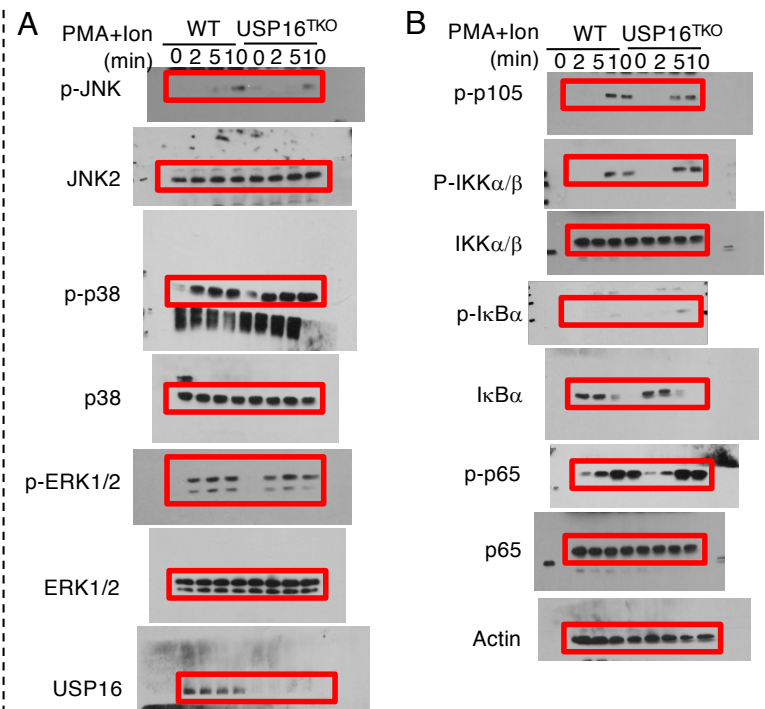
Full unedited gel for Supplementary Figure 2



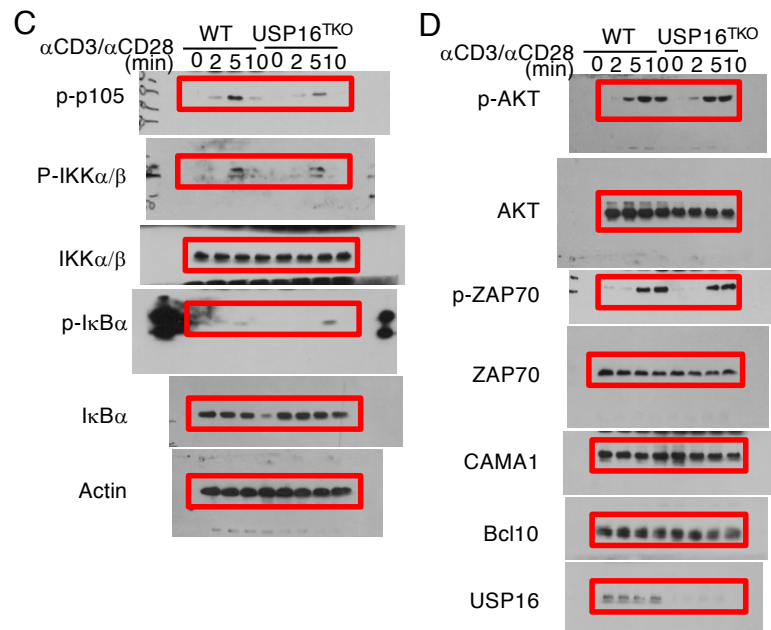
Full unedited gel for Supplementary Figure 2



Full unedited gel for Supplementary Figure 3



Full unedited gel for Supplementary Figure 3



Full unedited gel for Supplementary Figure 4

